Author Manuscript

Author Manuscript

Author Manuscript

Author Manuscript

HHS Public Access

Author manuscript

Bone. Author manuscript; available in PMC 2021 May 01.

Published in final edited form as:

Bone. 2020 May ; 134: 115269. doi:10.1016/j.bone.2020.115269.

Post-antibiotic gut dysbiosis-induced trabecular bone loss is dependent on lymphocytes

Naiomy Deliz Rios-Arce[1,2], **Jonathan D. Schepper**[2], **Andrew Dagenais**[2], **Laura Schaefer**[3], **Connor S. Daly-Seiler**[4], **Joseph D. Gardinier**[4], **Robert A. Britton**[3], **Laura R. McCabe**[2,5,6,7], **Narayanan Parameswaran**[1,2,7]

[1]Comparative Medicine and Integrative Biology Program, Michigan State University, East Lansing, Michigan, USA

[2]Department of Physiology, Michigan State University, East Lansing, Michigan, USA

[3]Department of Molecular Virology and Microbiology, Alkek Center for Metagenomics and Microbiome Research, Baylor College of Medicine, Houston, Texas, USA

[4]Henry Ford Health System-Bone and Joint Center

[5]Department of Radiology, Michigan State University, East Lansing, Michigan, USA

[6]Biomedical Imaging Research Center, Michigan State University, East Lansing, Michigan, USA

[7]These authors contributed equally to this work and are co-senior authors

Abstract

Recent studies in mouse models have shown that gut microbiota significantly influences bone health. We demonstrated that 2-week oral treatment with broad spectrum antibiotics followed by 4 weeks of recovery of the gut microbiota results in dysbiosis (microbiota imbalance)-induced bone loss in mice. Because gut microbiota is critical for the development of the immune system and since both microbiota and the immune system can regulate bone health, in this study, we tested the role of the immune system in mediating post-antibiotic dysbiosis-induced bone loss. For this, we treated wild-type (WT) and lymphocyte deficient Rag2 knockout (KO) mice with ampicillin/neomycin cocktail in water for 2 weeks followed by 4 weeks of water without antibiotics. This led to a significant bone loss (31% decrease from control) in WT mice. Interestingly, no bone loss was observed in the KO mice suggesting that lymphocytes are required for dysbiosis-induced bone loss. Bray-Curtis diversity metrics showed similar microbiota changes in both the WT and KO post-antibiotic treated groups. However, several operational taxonomic units (OTUs) classified as

Corresponding Authors: Narayanan Parameswaran (narap@msu.edu) and Laura R McCabe (mccabel@msu.edu).

Author contribution statement:

NDR-A devised and performed experiments, analyzed data, prepared figures and drafted manuscript. JS,AD, LS, CD-S, JG, RB, performed experiments and revised manuscript. NP, LM devised experiments, analyzed data, prepared figures and drafted and edited manuscript.

Publisher's Disclaimer: This is a PDF file of an unedited manuscript that has been accepted for publication. As a service to our customers we are providing this early version of the manuscript. The manuscript will undergo copyediting, typesetting, and review of the resulting proof before it is published in its final form. Please note that during the production process errors may be discovered which could affect the content, and all legal disclaimers that apply to the journal pertain.

Competing Interests:

None

Author Manuscript Author Manuscript Author Manuscript Author Manuscript

Lactobacillales were significantly higher in the repopulated KO when compared to the WT mice, suggesting that these bacteria might play a protective role in preventing bone loss in the KO mice after antibiotic treatment. The effect of dysbiosis on bone was therefore examined in the WT mice in the presence or absence of oral *Lactobacillus reuteri* treatment for 4 weeks (post-ABX treatment). As hypothesized, mice treated with *L. reuteri* did not display bone loss, suggesting a bone protective role for this group of bacteria. Taken together, our studies elucidate an important role for lymphocytes in regulating post-antibiotic dysbiosis-induced bone loss.

Keywords

Bone; probiotics; *Lactobacillus reuteri* 6475; adaptive immune system; microbiota

Introduction

Osteoporosis is characterized by low bone mass and altered bone architecture (1). Worldwide, this disease is estimated to affect more than 200 million people (2). In the US, osteoporosis accounts for over 2 million bone fractures with an estimated $17 billion treatment cost (3). By 2025, the annual costs associated with osteoporosis are estimated to increase by ~50% (4). Osteoporosis increases the risk for bone fractures that can lead to morbidity, mortality, loss of independence and decreased quality of life. Around 30% of people with hip fractures die during the first year and 50% have permanent disability (4). Many factors such as diet, age, sex, and medications can affect bone remodeling and lead to osteoporosis (5–9). Despite the development of new treatments against osteoporosis, patients are still concerned about drug effectiveness and unwanted side effects.

During the last decade, gut microbiota has emerged as an important regulator of host physiology including bone health. The gut microbiota comprises of ~1000 bacterial species of which the main phyla represented are Bacteroidetes, Firmicutes, Actinobacteria, Proteobacteria, and Verrucomicrobia (10). The intestinal microbiota is composed of both beneficial and harmful bacteria and thus, gut bacteria can be beneficial to the host as well as contribute to disease. For example, beneficial bacteria such as probiotics increase bone density (11–18) while pathogenic bacteria induce bone loss in animal models (19). Recent clinical studies further highlight the beneficial skeletal effects of ingesting probiotic bacteria in human subjects (20–22). Studies have also shown that imbalance in gut microbiota (dysbiosis) is involved in the pathogenesis of several diseases such as diabetes and obesity (23,24).

Although early studies in germ free mice implicated an important role for microbiota in bone health, subsequent studies demonstrated that the effect of microbiota on bone health could be influenced by age, sex, and strain of mice used in the studies. Another important variable that can significantly influence the effect of microbiota on bone health in germ free mouse studies is the composition of the gut microbiota used to conventionalize the germ-free mice. The composition of the mouse gut microbiota can be different between facilities, age, and mouse strain and thus can affect host functions differentially (14,25–28). More importantly, studies in germ free mice are further complicated due to the developmental

Author Manuscript Author Manuscript Author Manuscript Author Manuscript

defects in the immune system (25,29). To better understand the role of the gut microbiota on bone density, our lab and others have used antibiotics to deplete commensal microbiota. Our lab recently demonstrated that administration of the broad spectrum antibiotics (ampicillin and neomycin) followed by natural gut microbiota repopulation for four weeks leads to dysbiosis and reduced trabecular femoral bone density (30). This experimental approach is especially useful to understand gut dysbiosis effects on bone density and is distinct from studies that have utilized either germ-free mice or have focused on chronic antibiotic treatment (26,31–33).

The gut-bone signaling mechanisms that account for microbiota regulation of bone density are not fully understood but are thought to involve: improvement of intestinal barrier function (30), alteration of metabolic hormone levels (26), changes in nutrient absorption (34), regulation of the immune system (15,17,35,36), and microbial byproduct regulation of host cell functions (37). Our lab and others have shown that oral treatment with probiotics can influence the immune system as well as increase bone density in several different mouse models (14,15,17,36,38). In fact, recent studies have shown that microbiota metabolites can enhance bone health via regulation of T-regulatory lymphocytes (36). These data suggest a critical role for the immune system in gut microbiota regulation of bone density. In this study, we aimed to identify the requirement of T and B lymphocytes in dysbiosis-induced bone loss in the antibiotic-induced dysbiosis model in mice. Using mice deficient in mature T and B lymphocytes (Rag2 knockout), we demonstrate an important link between the gut microbiota and the lymphocytes in the modulation of bone density following antibiotic-induced dysbiosis.

Materials and methods

Animals and Experimental design

Wild-type (C57BL/6) and Rag2 knockout ($Rag2^{tm1Mom}$, C57BL/6 background) male mice were originally purchased from The Jackson Laboratory (Bar Harbour, Maine) and bred in-house. Both strains of mice were housed in the same room and on the same rack to ensure adaptation to identical housing environment and to prevent cage effect. At 12 weeks of age male mice were randomly divided into 4 experimental groups: 1) WT and 2) KO control groups that received water and 3) WT and 4) KO antibiotic groups that received antibiotics in water. The antibiotics ampicillin 1.0 g/L (Sigma, St. Louis, MO) and neomycin 0.5 g/L (Sigma, St. Louis, MO) were used to deplete the gut microbiota (30,39,40) and were given in the drinking water for 2-weeks. The drinking water, with or without antibiotics, was renewed every week. Antibiotic depletion of the gut microbiota was confirmed by the lack of fecal bacterial growth on agar plates as explained below. After 2-weeks, the antibiotic treatment ceased, and mice were treated for 4-weeks with water alone or water containing *Lactobacillus reuteri* 6475 (LR) (for culture and supplementation see next paragraph). Mice were euthanized 4-weeks after cessation of antibiotic treatment (at age 18 weeks). During the study mice were given Teklad 7914 chow (Madison, WI) and water ad libitum. Mice were housed in a 12:12-h light-dark cycle at 23°C in groups of up to 4 animals per cage. All animal procedures were approved by the Michigan State University Institutional Animal Care and Use Committee (IACUC) and conformed to NIH guidelines.

Author Manuscript Author Manuscript Author Manuscript Author Manuscript

Culture and Supplementation of *L. reuteri*:

Lactobacillus reuteri ATCC PTA 6475 was cultured in deMan, Rogosa, Sharpe media (MRS, Difco) agar plates and kept under anaerobic conditions overnight at 37°C. The next day, 1 μl full loop of bacteria were sub-cultured into 10 ml of fresh MRS broth for 16–18 hours anaerobically at 37°C. The overnight culture was then sub-cultured anaerobically at 37°C in fresh MRS broth and grown until log phase (OD600 =0.4). *L. reuteri* 6475 was then pelleted by centrifugation at 4000 RCF for 10 minutes and washed 3 times with 1 X sterile phosphate-buffered saline (PBS). The final pellet was re-suspended in 60 ml sterile PBS and one milliliter (ml) aliquots were made and stored at −80°C until use. Colony-forming units per milliliter (cfu/ml) were calculated the day before treatment by plating 10 μl of the aliquots into MRS agar plates overnight at 37°C. Mice were treated with 3.3×10^8 cfu/ml of *L. reuteri* 6475 in the drinking water. Three times per week the drinking water was refilled with fresh water +/− probiotic.

Bacterial cultivation of feces

After two weeks of antibiotic treatment, fresh fecal samples were collected, weighed and then resuspended in 1 ml sterile PBS. Several dilutions were performed and 10 μl of the fecal suspension was plated-on Luria broth base agar plates (LB, Invitrogen). Plates were then incubated aerobically and anaerobically at 37° C for 24 hours. At the end of the incubation period, the number of colonies on the plates were counted, and the number of bacteria per gram of feces was calculated.

Microcomputed tomography (μCT) bone imaging

Femoral bone was collected at the day of harvest and fixed in 10% formalin for 24 hours. Bones were transferred to 70% ethanol and scanned using a GE Explore Locus microcomputed tomography (μCT) system at a voxel resolution of 20 μm obtained from 720 views. Each run included bones from mice of each experimental condition, as well as a calibration phantom to standardize gray scale values and maintain consistency across analyses. A fixed threshold (841) was used to separate bone from the bone marrow. Femur trabecular bone analyses were performed from 1% of the total length proximal to the growth plate, extending 10% of bone length toward the diaphysis, and excluding the outer cortical bone. Trabecular bone volume fraction (BVF), bone mineral content (BMC), bone mineral density (BMD), thickness (Tb. Th), spacing (Tb. Sp), and number (Tb. N) were computed using GE Healthcare MicroView software. Femoral trabecular isosurface images were taken from a region in the femur where analyses were performed measuring 1.0 mm in length and 1.0 mm in diameter. Cortical measurements were performed in a 2- × 2- × 2 mm cube region of interest centered midway down the length of the bone. All bone analyses were done blinded to the experimental conditions.

Serum measurements

Sterile blood was collected at the end of the study and was allowed to clot at room temperature for 5 minutes and then centrifuged at 5000g for 10 minutes. Serum was removed and 30 μl were aliquoted and snap frozen in liquid nitrogen and stored at −80°C. Serum samples did not go through more than 1 freeze/thaw cycle. Serum osteocalcin (OC)

Author Manuscript Author Manuscript Author Manuscript Author Manuscript

and tartrate-resistant acid phosphatase (TRAP5b) were measured using a mouse OC and TRAP5b assay kits (BT – 470, Biomedical Technologies Inc., Stoughton, MA, and SB-TR103; Immunodiagnostic Systems Inc., Fountain Hills, AZ) respectively by the manufacturer's protocol.

DNA preparation of fecal samples

DNA for microbial sequence analysis was extracted from mouse fecal samples by bead-beating and modified extraction with Qiagen DNeasy Blood and Tissue kits as described previously (17,28). As previously described (30) fecal samples were transferred to Mo Bio Ultra Clean Fecal DNA bead Tubes (MoBio) containing 360µl of buffer ATL (Qiagen) and homogenized for one minute in a BioSpec Mini-Beadbeater. 40µL proteinase K (Qiagen) was added and samples were incubated for 30 minutes at 55°C, then homogenized again for one minute and incubated at 55°C for additional 30 minutes. DNA was extracted with Qiagen DNeasy Blood and Tissue kit.

16S rRNA gene amplification, and sequencing

Bacterial 16S sequences spanning variable region V4 were amplified by PCR with primers F515/R806 with a dual indexing approach and sequenced by Illumina MiSeq described previously (41). PCR reactions (20 µl) were prepared in duplicate and contained 40ng DNA template, 1X phu-sion high-fidelity buffer (New England Biolabs), 200 µMdNTPs (Promega or Invitrogen), 10 nM primers, 0.2 units of Phu- sion DNA Polymerase (New England Biolabs), and PCR grade. Reactions were performed in an Eppendorf Pro thermal cycler with an initial denaturation at 98 °C for 30 s, followed by 30 cycles of 10 s at 98 °C, 20 s at 51 °C, and 1 min at 72 °C. Replicates were pooled and purified with Agencourt AMPure XP magnetic beads (Beckman Coulter). DNA samples were quantified using the QuantIt High Sensitivity DNA assay kit (Invitrogen) and pooled at equilmolar ratios. The quality of the pooled sample was evaluated with the Bioanalyzer High Sensitivity DNA Kit (Agilent).

Microbial community analysis

Sequence data was processed using the MiSeq pipeline for mothur using software version 1.38.1 (42) as described previously (28). In brief, forward and reverse reads were aligned, sequences were quality trimmed and aligned to the Silva 16S rRNA gene reference database formatted for mothur, and chimeric sequences were identified and removed using the mothur implementation of UCHIME. Sequences were classified according to the mothur-formatted Ribosomal Database Project (version 16, February 2016) using the Bayesian classifier in mothur, and those sequences classified as Eukarya, Archaea, chloroplast, mitochondria, or unknown were removed. The sequence data were then filtered to remove any sequences present only once in the data set. After building a distance matrix from the remaining sequences with the default parameters in mothur, sequences were clustered into operational taxonomic units (OTUs) with 97% similarity using the average-neighbor algorithm in mothur. 871 OTUs were identified across all samples with an average rarefaction depth of 54,791 reads per sample. Alpha and beta diversity analyses and visualization of microbiome communities were performed with the statistical software R, utilizing the phyloseq package (43,44). The Bray-Curtis dissimilarity matrix was used to describe differences in microbial community structure. Analysis of similarity (ANOSIM) was performed in mothur. Shannon

Author Manuscript Author Manuscript Author Manuscript Author Manuscript

alpha diversity indices were calculated using an OTU cutoff of 97% similarity and tested for overall significance using Kruskal-Wallis analysis with adjustment for false discovery rate. Pairwise comparisons were then tested for significance using the Mann-Whitney U test, a nonparametric test that compares differences between groups that are not normally distributed, and p-values were adjusted for an 0.05% false discovery rate. Adjusted p-values of less than 0.005 were considered significant. Analysis of similarity (ANOSIM) was performed in mothur with p-values of less than 0.05 considered significant.

Mechanical Testing

Via microCT imaging the $I_{A/P}$ and c were determined at the site of fracturing as described above. Mechanical properties of the mouse tibias were determined under four-point bending using an EnduraTech ELF 3200 Series (Bose®, MA) (45). The base support span was 9mm with a load span of 3mm. The tibia was positioned in the loading device so the medial surface was in tension by placing the most distal portion of the tibia and fibula junction directly over the left-most support. Each tibia was loaded at 0.01 mm/s until failure, while the load and displacement were recorded. The force-deflection curve was used to calculate the structural-level properties, while tissue-level properties were estimated using the following beam-bending equations: Stress = $\sigma = f \cdot a \cdot c / 2 \cdot I_{A/P}$; Strain = $\varepsilon = 6 \cdot c \cdot d / a (3 \cdot L - 4 \cdot a)$. In each equation, f is the applied force, d is the resulting displacement, a is the distance between the inner spans (3mm), L is the distance of the outer spans (9mm), $I_{A/P}$ is the moment of inertia about the anterior/posterior axis, and c is the distance from the neutral axis to the medial surface under tension. The yield point was determined from the stress-strain relationship using a 20% offset method (46). Analyses were done blind to the experimental condition of the sample.

Statistical analysis

All measurements are presented as the mean ± standard error. To determine statistical significance between the groups One-way ANOVA followed by Tukey post hoc test (more than 2 groups) and T-test (for two groups) was performed using GraphPad Prism software version 7 (GraphPad, San Diego, CA, USA). Significant outliers (if present and indicated in figure legend) were removed using the ROUT test (Q=0.1%) for outliers. A p-value ≤ 0.05 was considered significant and <0.01 highly significant.

Results

Two week-broad spectrum antibiotic treatment depletes fecal microbiota in mice

Oral treatment of mice with the broad-spectrum antibiotics (ABX) ampicillin and neomycin has been shown to deplete gut microbiota (30,39,40,47–49). We used these two specific antibiotics because they are poorly absorbed in the mouse gut, thereby limiting extra-intestinal effects (50–52). Twelve-week-old wild type (WT) and Rag2 knockout (KO) male mice were treated for two weeks with ABX (ampicillin: 144 mg/kg/day and neomycin: 72.46 mg/kg/day) in the drinking water (Figure 1A). Microbiota depletion in the ABX groups was confirmed by plating fecal samples on Luria broth agar plates and incubating for 24 hours under aerobic and anaerobic conditions. Our results demonstrated no colony formation in any of the ABX treated groups (Figure 1B). ABX treated mice were allowed to

Author Manuscript Author Manuscript Author Manuscript Author Manuscript

repopulate for 4 weeks, following the 2-week ABX treatment (Figure 1A). General body parameters were assessed at 4-week post-ABX time point at which mice were euthanized and various organs harvested. Cecum weights in both WT and KO groups were increased in the post-ABX groups compared to the control groups (Table 1). As expected, a significant decrease in spleen weight was observed in the KO compared to the WT mice (53). Other parameters such as body weight, liver, and kidney weights did not statistically differ between the various groups (Table 1).

Post-ABX dysbiosis-induced bone loss is abrogated in Rag2 KO mice

We recently demonstrated that natural gut microbiota repopulation for four weeks after broad spectrum ABX treatment causes dysbiosis and decreases bone density in BALB/c male mice (30). To examine if these effects are mouse strain specific as well as to determine the role of lymphocytes in post-ABX dysbiosis-induced bone loss we used Rag2 knockout (deficient in T and B lymphocyte) and their corresponding wild type mice, both in C57BL/6 background. We first determined the microbiota composition following repopulation to confirm dysbiosis in post-ABX groups (both genotypes). Microbiota composition in colonic fecal samples was examined by 16S rRNA analysis. Similar to our previous study, antibiotic treatment increased gut microbiota dysbiosis (as described by increased Firmicutes:Bacteroidetes ratio) in both WT and KO groups (Figure 1C, **$p<0.05$**).

Femoral bone showed a significant decrease (31%) in trabecular bone density in WTABX mice compared to non-ABX group (Figure 2A, **$p<0.05$**). Consistent with these findings, trabecular thickness decreased (Tb. Th, $p<0.05$), while trabecular space increased (Tb. Sp, $p<0.05$) in the WT-ABX treated group compared to the WT untreated mice (Figure 2B, Table 2). Interestingly, gut microbiota repopulation did not affect trabecular femoral bone density in the KO-ABX group, suggesting that lymphocytes are important in microbiota-induced bone loss (Figure 2A). No significant changes in trabecular thickness or space were observed in the Rag2 KO groups. We also analyzed the diaphyseal region of the femur and did not find any significant differences between the groups (Table 2) indicating that post-ABX microbiota repopulation does not affect cortical bone at this timepoint in either of the genotypes.

To determine whether the post-ABX microbiota affects catabolic or anabolic bone parameters we measured serum markers of bone remodeling. Levels of tartrate-resistant acid phosphatase (TRAP 5b), a marker of bone resorption, were modestly increased in the WT-ABX group compared to control. (Figure 2C). Osteocalcin (OC) levels, a marker of osteoblast activity/bone formation, were significantly lower in the WT-ABX treated group (Figure 2C, **$p<0.05$**). No changes in the KO-ABX group were observed in either of these serum markers. Taken together, our results suggest that gut microbiota repopulation following ABX treatment regulates bone density by primarily affecting bone anabolic processes in C57Bl/6 mouse strain and this effect requires the presence of T and B lymphocytes.

Author Manuscript Author Manuscript Author Manuscript Author Manuscript

Gut dysbiosis does not alter mechanical bone properties

Gut microbiota manipulations can lead to changes in structural and tissue levels properties. Therefore, we investigated whether 4-week post-antibiotic WT and KO mice display differences in tibia bone mechanical properties. Comparisons across all the groups showed no significant changes in structural (Figure 3A) and tissue level mechanical properties (Figure 3B). These results suggest that natural repopulation for four weeks after ABX does not affect the overall strength and tissue properties of the cortical bone in C57BL/6 male mice.

Antibiotic-induced dysbiosis leads to different microbial communities in WT and KO mice.

To further examine if differences in microbiota between WT and KO mice can explain part of the mechanisms underlying the different phenotype, we analyzed microbial communities from fecal samples by beta diversity metrics (Bray-Curtis) and alpha diversity (Shannon diversity) (Figure 4A–B). We determined the differences among our samples by calculating the pairwise differences of samples, a distance matrix, using the Bray-Curtis dissimilarity metric and reduced these data for display in a Principle Coordinate Analysis (Fig 4A). Analysis of colonic fecal samples by beta diversity metrics (Bray-Curtis) showed statistically significant separation between WT and WT-ABX (Figure 4A, **R=0.233498, p=0.001)** and KO and KO-ABX treated mice (Figure 4A, **R=1, p<0.001)**. No significant changes were found between the WT-ABX and KO-ABX groups by diversity metrics (Bray-Curtis) (Figure 4A, **R=0.0446297, p=0.209)**. However, pairwise comparison of WT and KO mice showed a significant separation (R=0.5895; p<0.001). Furthermore, Shannon diversity analysis showed that antibiotics significantly reduced diversity as expected (Fig. 4B). In addition, the Rag2 KO mice had significantly higher diversity than the WT mice; however, since the WT and Rag2 KO mice were not littermates it is not possible to conclude this is solely due to the knockout of Rag2.

We next analyzed specific bacterial OTUs at the phylum, class, and order levels, to assess differences between the various groups/treatments (Figure 5). While the trends were similar, the post-ABX-induced OTU shift, in terms of the relative abundance of several bacteria, was significantly different between the WT versus the KO groups. At the phylum level our data show a significant decrease in the relative abundance of Bacteroidetes in WT-ABX groups (Figure 5A, **p<0.001)** that was further decreased to almost undetectable levels in the KO-ABX group (Figure 5A, **p<0.0001)**. This pattern was seen for bacteria in the class (Bacteroidia, 5B), and order (Bacteroidales, 5C). The other commonly altered phylum, Firmicutes, showed no changes after ABX treatment in any of the groups (Figure 5A), however, the KO-ABX group showed dramatic increases in bacteria in the class (Bacilli, **p<0.0001**, 5B) and order (Lactobacillales, **p<0.0001**, 5C). Additionally, the relative abundance of Verrumicrobia phylum was higher in WT-ABX treated groups and further higher in the KO-ABX mice (Figure 5A, **p<0.0001)**, with bacteria in the class (Verrumicrobiae, 5B), and order (Verrucomicrobiales, 5C) following this pattern. The phylum Actinobacteria composed a small part (<1%) of the total bacteria composition and was decreased by ABX treatment. Together, these data suggest that the abundance of several OTUs is different between the WT-ABX and KO-ABX groups.

Author Manuscript Author Manuscript Author Manuscript Author Manuscript

Lactobacillus reuteri administration prevents post-antibiotic dysbiosis-induced bone loss in wild type mice

As indicated in figure 5C, the relative abundance of Lactobacillales is markedly increased in the KO-ABX compared to WT-ABX treated mice. To test if increasing the levels of Lactobacillaes in the WT-ABX group could result in a bone phenotype similar to WT control group, we supplemented WT-ABX group with *Lactobacillus reuteri* 6475 for four weeks. Note that these experiments were performed together with the experiments shown in Figure 2. Also, the choice of Lactobacillus (*L. reuteri 6475*) is based on our previous studies in Balb/C mice showing a protective effect on bone following ABX-dysbiosis. Compared to the significant decrease in bone density observed in WT-ABX mice that did not receive *L. reuteri*, bone loss was prevented in WT-ABX group treated with *L. reuteri* (Figure 6A, $p<0.05$). Consistent with BVF results, treatment with *L. reuteri* decreased trabecular space (Figure 6B, $p<0.05$) and increased trabecular number (Figure 6B, $p<0.05$). An increase in osteocalcin levels in the serum was also evident in the post-ABX *L. reuteri*-treated group (Figure 6C, $p<0.05$). We also examined the relative abundance of *L. reuteri* and found a significant increase in the post-ABX *L. reuteri* treated group (Figure 6D, $p<0.05$). Microbiota analysis by Bray-Curtis PCoA revealed significant separation overall but the communities were not very different from each other between WT-ABX VS WT-ABX-LR ($R=0.18661$; $p=0.001$). Note however that, WT-ABX-LR and WT-none were most different ($R=0.816$; $p=<0.001$). Together, these data suggest that: 1) changes in post-ABX gut microbiota composition between WT and KO, specifically an increase in *Lactobacillales* in the KO-ABX group, could contribute to the difference in bone response, and 2) four weeks of post-antibiotic treatment with *L. reuteri* prevents bone loss in C57Bl/6 strain, similar to BALB/c (30).

Discussion

Antibiotics are widely prescribed for the treatment and prevention of bacterial infections. Several studies have shown that antibiotics can also deplete the commensal flora in the host, leading to bacterial disturbances and long-term changes that can have sustained negative impact on the host (54–59). We recently demonstrated that gut microbiota repopulation for 4 weeks following 2-weeks of antibiotic treatment (post-ABX) causes microbial dysbiosis and significantly decreases femoral trabecular bone density in BALB/c male mice (30). Our model to assess the role of the gut microbiota on bone density uses the antibiotics ampicillin and neomycin. These antibiotics were chosen because they are poorly absorbed in the rodent intestine(50–52) and they can also deplete the intestinal microbiota (39,40). Importantly, our lab has shown that two weeks treatment with these antibiotics does not significantly affect trabecular bone density (30), suggesting that these antibiotics do not have direct effect on bone density. In the present study we identify lymphocytes as one of the key players involved in post-ABX dysbiosis-induced bone loss in C57BL/6 male mice. We also identified *Lactobacillus* supplementation as a possible approach for preventing adverse bone effects following ABX-induced gut dysbiosis. Our studies in C57BL/6 strain also confirm previous findings in BALB/c strain, suggesting that gut dysbiosis-induced bone loss may not be mouse strain-specific. However, given the differences in microbiota composition between different strains (as well as other strain related variables) the mechanisms of dysbiosis-

Author Manuscript Author Manuscript Author Manuscript Author Manuscript

induced bone loss may not be identical between the two strains. For example, in Balb/c mice we showed that antibiotic-induced bone loss is accompanied by both a decrease in osteocalcin as well as an increase in TRAP5b. While in the current study C57BL/6J mice displayed a decrease in osteocalcin that is similar to Balb/c, the increase in TRAP5b is not as marked as in the Balb/c strain. Whether this is due to different mechanisms of bone loss will be the subject of future studies.

The effect of T and B lymphocytes and their cytokines on bone density is well known. These cells regulate bone density through the secretion of cytokines or via direct cell-cell contact with osteoblasts or osteoclasts (60–62). Cytokines such as IFN-γ, TNF-α, and interleukin-17 (IL-17) are mostly associated with bone loss, mainly through their effects in promoting osteoclastogenesis but preventing osteoblastogenesis (63–67). In contrast, T regulatory cells (Treg) and interleukin 10 (IL-10) modulate bone density by enhancing osteoblastogenesis but inhibiting osteoclastogenesis (68–70). We and others have demonstrated that different probiotic bacteria can regulate the immune system which is associated with beneficial effects on bone. For example, *in vivo*, the probiotic *L. reuteri* decreases TNFα gene expression in the jejunum and ileum, and $CD4^+$ T cells in the bone marrow and these effects are associated with increased bone density (15,17). Furthermore, we demonstrated recently that beneficial effect of *L. reuteri* on bone density in male mice is dependent on lymphocytes (71). Intriguingly, in female mice *L. reuteri* requires an elevated inflammatory status to enhance bone density (18). Other probiotics such *Lactobacillus rhamnosus* (LGG) and VSL#3 can decrease intestinal and bone marrow inflammation and can also enhance bone density (14). Interestingly, in a recent study LGG effects on bone density were demonstrated to be mediated by the T-regs (36). An increase in Tregs by LGG was shown to enhance $CD8^+$ T cells which were then shown to promote bone formation via the Wnt pathway (36). Another study using *Lactobacillus acidophilus* (LA) was shown to increase bone density in OVX mice by inhibiting osteoclastogenic Th17 cells and promoting anti-osteoclastogenic T-reg cells, thus regulating T-reg-Th17 balance (38). Owing to the fact that different bacteria can regulate the immune system with associated benefits on bone, in this study we were interested to see if the negative effects on post-ABX dysbiosis on bone density were mediated by lymphocytes. Our studies clearly demonstrate that absence of T and B lymphocytes inhibits post-ABX dysbiosis-induced bone loss.

Antibiotics have been used previously to study their effects on bone in different animal models. However, unlike our model, these studies were mainly done in young mice and used chronic antibiotic treatment. Cho et al showed that female mice (C57BL/6J) treated chronically with antibiotics for three weeks exhibited a significant increase in BMD, while long term use of the antibiotics (7 weeks) did not have any effect (31). Other studies have also shown that chronic treatment (20 weeks) with low dose of penicillin at birth or at weaning in C57BL/6J female mice increases BMD. Intriguingly, male mice treated with the same low dose of penicillin presented a decrease in bone mineral content when the treatment began at birth (32). Guss et al showed that male mice (C57BL/6J) treated with ampicillin and neomycin from weaning until skeletal maturity (16 weeks old) exhibit a decrease in femoral cortical area, thickness, and bone bending strength (33). In contrast, 2-month old female BALB/c mice treated with antibiotic for one month showed an increase in bone density (26). Together, these studies suggest that antibiotic use affects bone density and this

Author Manuscript Author Manuscript Author Manuscript Author Manuscript

effect is variable depending on several factors including class of antibiotic, dose, treatment duration, sex, age, and strain of the animal. It is important to note that while our model utilized antibiotics to deplete gut bacteria, the effect on bone density was observed in response to changes in gut repopulation, rather than direct effect of antibiotics *per se*. Because we examined bone responses 4 weeks following cessation of ABX treatment, our results likely rule out direct effect of ABX on bone.

Several studies have shown that antibiotic use can lead to changes in gut microbiota composition (dysbiosis), which in some cases can take years to revert to the original configuration (72–75). Previously, using the same model but in a different strain of mice we found that antibiotic treatment leads to microbial dysbiosis (30). In this study using a different strain of mice, treatment with ABX led to microbial dysbiosis that appeared similar (based on Firmicutes:Bacteriodetes ratio) between WT and Rag2-KO mice. Interestingly, by Bray-Curtis analysis we did not see significant differences in gut microbial composition between the WT and KO group after ABX treatment. However, when we looked at specific OTUs, the relative abundance of several bacteria was expressed differentially between the WT and KO mice following post-ABX repopulation. This data is consistent with other studies that have shown that different bacteria are present in the WT and Rag2 KO mice (76,77). One result that should be underscored was the increase in the relative abundance of Lactobacillales in the KO-ABX treated group. Lactobacillales belongs to the Firmicutes phylum which comprise one of the most common phyla of bacteria in the gut. In addition, several studies from our group and others have shown beneficial effects on bone density by treatment with different species of Lactobacillales (14,17,18,30,78,79). Indeed, when we treated WT mice with *L. reuteri* 6475 for four weeks after antibiotic treatment we were able to prevent the decrease in bone density induced by gut microbiota repopulation. These results suggest that Lactobacillales repopulation in the KO ABX group might be protective and could explain the lack of bone loss in the KO mice. It should however be noted that the relative abundance of other bacteria also changed between the groups and further extensive studies are needed to confirm the contribution of each of these bacteria in protecting against bone loss in the wild type mice. Similarly, not all Lactobacillus species are effective in preventing dysbiosis-induced bone loss. Our studies in multiple models of bone loss suggest that *L. reuteri* is better than *L. rhamnosus GG (LGG)* (30,80). Others have shown beneficial effects of different Lactobacillus species (including LGG) in estrogen deficiency-induced bone loss(79,81). These studies support the importance of individual bacterial strains in mediating bone health depending on the pathogenesis of bone loss.

Previous studies in germ free mice suggest that gut microbiota can influence bone health. However, the specific effects are dependent on the source of microbiota for conventionalization as well as the strain, sex and age of the mice. Interestingly, conventionalization of female C57BL/6 germ-free mice with microbiota resulted in loss of femoral trabecular and cortical bone and this was associated with an increase in osteoclastogenic $CD4^+$ T cells in the bone marrow, suggesting a link between microbiota, immune system and bone (14). In our studies here, we provide further demonstrative evidence using knockout mice that lymphocytes are critical in mediating microbiota effects on bone. Although our studies are consistent with these studies in germ-free mice, comparing our results with the studies in germ-free mice should be done with caution as

Author Manuscript Author Manuscript Author Manuscript Author Manuscript

germ-free mice do not have a fully mature immune system and these differences can directly affect bone formation (14,82).

In summary, in this study we demonstrate a role for lymphocytes in mediating microbiota effects on bone density following ABX-induced dysbiosis. How microbiota repopulation is influenced by the immune system, especially the lymphocytes and the specific cell types involved in this process will be the subject of future studies.

Acknowledgements:

The authors thank the staff of Campus Animal Resources for the excellent care of our animals. The work presented in this study was funded in part by the National Institute of Health, grants AT007695 (to LRM, RAB and NP), and DK101050 (to LRM and NP); NDR-A was supported by the William Townsend Porter Pre- doctoral Fellowship from the American Physiological Society.

Funding:

The work presented in this study was funded in part by NIH AT007695 (to RAB, LRM and NP), and DK101050 (to LRM and NP); NDR-A was supported by the William Townsend Porter Pre-doctoral Fellowship from the American Physiological Society.

References:

1. Kanis JA, Glüer CC. An update on the diagnosis and assessment of osteoporosis with densitometry. Committee of Scientific Advisors, International Osteoporosis Foundation. Osteoporos Int. 2000;11(3):192–202. [PubMed: 10824234]
2. Reginster JY, Burlet N. Osteoporosis: A still increasing prevalence. Bone. 2006;38(2 SUPPL. 1):1998–2003.
3. Burge R, Dawson-Hughes B, Solomon DH, Wong JB, King A, Tosteson A. Incidence and economic burden of osteoporosis-related fractures in the United States, 2005–2025. J Bone Miner Res. 2007 3;22(3):465–75. [PubMed: 17144789]
4. Burge R, Dawson-Hughes B, Solomon DH, Wong JB, King A, Tosteson A. Incidence and Economic Burden of Osteoporosis-Related Fractures in the United States, 2005–2025. J Bone Miner Res. 2006;22(3):465–75.
5. Sahni S, Mangano KM, McLean RR, Hannan MT, Kiel DP. Dietary approaches for bone health: lessons from the Framingham Osteoporosis Study. Curr Osteoporos. 2015;(4):368–79.
6. Demontiero O, Vidal C, Duque G. Aging and bone loss: new insights for the clinician. Ther Adv Musculoskelet Dis. 2012 4;4(2):61–76. [PubMed: 22870496]
7. Ibanez L, Rouleau M, Wakkach A, Blin-Wakkach C. Gut microbiome and bone. Jt Bone Spine. 2017;000(2017):1–6.
8. Hernandez CJ, Guss JD, Luna M, Goldring SR. Links Between the Microbiome and Bone. J Bone Miner Res. 2016 9;31(9):1638–46. [PubMed: 27317164]
9. Pacifici R Bone Remodeling and the Microbiome. Cold Spring Harb Perspect Med. 2017;1–20.
10. Huttenhower C, Gevers D, Knight R, Abubucker S, Badger JH, Chinwalla AT, et al. Structure, function and diversity of the healthy human microbiome. Nature. 2012 6;486(7402):207–14. [PubMed: 22699609]
11. Parvaneh K, Ebrahimi M, Sabran MR, Karimi G, Hwei ANM, Abdul-Majeed S, et al. Probiotics (*Bifidobacterium longum*) Increase Bone Mass Density and Upregulate *Sparc* and *Bmp-2* Genes in Rats with Bone Loss Resulting from Ovariectomy. Biomed Res Int. 2015;2015:1–10.
12. Parvaneh K, Jamaluddin R, Karimi G, Erfani R. Effect of probiotics supplementation on bone mineral content and bone mass density. Sci World J. 2014;2014:1–6.
13. Scholz-Ahrens KE, Adolphi B, Rochat F, Barclay DV., de Vrese M, Açil Y, et al. Effects of probiotics, prebiotics, and synbiotics on mineral metabolism in ovariectomized rats - impact of bacterial mass, intestinal absorptive area and reduction of bone turn-over. NFS J. 2016 8;3:41–50.

Author Manuscript Author Manuscript Author Manuscript Author Manuscript

14. Li J-Y, Chassaing B, Tyagi AM, Vaccaro C, Luo T, Adams J, et al. Sex steroid deficiency-associated bone loss is microbiota dependent and prevented by probiotics. J Clin Invest. 2016 6;126(6):2049–63. [PubMed: 27111232]
15. McCabe LR, Irwin R, Schaefer L, Britton R a. Probiotic use decreases intestinal inflammation and increases bone density in healthy male but not female mice. J Cell Physiol. 2013 8;228(8):1793–8. [PubMed: 23389860]
16. Zhang J, Motyl KJ, Irwin R, MacDougald O a., Britton R a., McCabe LR. Loss of bone and Wnt10b expression in male type 1 diabetic mice is blocked by the probiotic L. reuteri. Endocrinology. 2015;(July):EN20151308.
17. Britton RA, Irwin R, Quach D, Schaefer L, Zhang J, Lee T, et al. Probiotic L. reuteri Treatment Prevents Bone Loss in a Menopausal Ovariectomized Mouse Model. J Cell Physiol [Internet]. 2014;229(11):1822–30. Available from: http://www.ncbi.nlm.nih.gov/pubmed/24677054
18. Collins FL, Irwin R, Bierhalter H, Schepper J, Britton RA, Parameswaran N, et al. Lactobacillus reuteri 6475 increases bone density in intact females only under an inflammatory setting. PLoS One [Internet]. 2016;11(4):e0153180 Available from: http://www.ncbi.nlm.nih.gov/pubmed/27058036
19. Irwin R, Lee T, Young VB, Parameswaran N, McCabe LR. Colitis-induced bone loss is gender dependent and associated with increased inflammation. Inflamm Bowel Dis. 2013;19(8):1586–97. [PubMed: 23702805]
20. Jafarnejad S, Djafarian K, Fazeli MR, Yekaninejad MS, Rostamian A, Keshavarz SA. Effects of a Multispecies Probiotic Supplement on Bone Health in Osteopenic Postmenopausal Women: A Randomized, Double-blind, Controlled Trial. J Am Coll Nutr. 2017;36(7):497–506. [PubMed: 28628374]
21. Nilsson AG, Sundh D, Bäckhed F, Lorentzon M. *Lactobacillus reuteri* reduces bone loss in older women with low bone mineral density - a randomized, placebo-controlled, double-blind, clinical trial. J Intern Med. 2018;0–3.
22. Laird E, Molloy AM, McNulty H, Ward M, McCarroll K, Hoey L, et al. Greater yogurt consumption is associated with increased bone mineral density and physical function in older adults. Osteoporos Int. 2017;28(8):2409–19. [PubMed: 28462469]
23. Baothman OA, Zamzami MA, Taher I, Abubaker J, Abu-Farha M. The role of Gut Microbiota in the development of obesity and Diabetes. Vol. 15, Lipids in Health and Disease. BioMed Central; 2016 p. 108.
24. Blandino G, Inturri R, Lazzara F, Di Rosa M, Malaguarnera L. Impact of gut microbiota on diabetes mellitus Vol. 42, Diabetes and Metabolism. Elsevier Masson; 2016 p. 303–15. [PubMed: 27179626]
25. Sjögren K, Engdahl C, Henning P, Lerner UH, Tremaroli V, Lagerquist MK, et al. The gut microbiota regulates bone mass in mice. J Bone Miner Res. 2012 6;27(6):1357–67. [PubMed: 22407806]
26. Yan J, Herzog JW, Tsang K, Brennan CA, Bower MA, Garrett WS, et al. Gut microbiota induce IGF-1 and promote bone formation and growth. Proc Natl Acad Sci. 2016;113(47):E7554–63. [PubMed: 27821775]
27. Novince CM, Whittow CR, Aartun JD, Hathaway JD, Poulides N, Chavez MB, et al. Commensal Gut Microbiota Immunomodulatory Actions in Bone Marrow and Liver have Catabolic Effects on Skeletal Homeostasis in Health. Sci Rep. 2017;7(1):5747. [PubMed: 28720797]
28. Quach D, Collins F, Parameswaran N, McCabe L, Britton RA, Bidwell J, et al. Microbiota Reconstitution Does Not Cause Bone Loss in Germ-Free Mice. mSphere [Internet]. 2018 2;3(1):e00545–17. Available from: http://www.ncbi.nlm.nih.gov/pubmed/29299532%0Ahttp://www.pubmedcentral.nih.gov/articlerender.fcgi?artid=PMC5750390%0Ahttp://msphere.asm.org/lookup/doi/10.1128/mSphereDirect.00545-17
29. Schwarzer M, Makki K, Storelli G, Machuca-Gayet I, Srutkova D, Hermanova P, et al. Lactobacillus plantarum strain maintains growth of infant mice during chronic undernutrition. Science (80-). 2016;351(6275).

Author Manuscript Author Manuscript Author Manuscript Author Manuscript

30. Schepper JD, Collins FL, Rios-Arce ND, Raehtz S, Schaefer L, Gardinier JD, et al. Probiotic Lactobacillus reuteri Prevents Postantibiotic Bone Loss by Reducing Intestinal Dysbiosis and Preventing Barrier Disruption. J Bone Miner Res. 2019 1;

31. Cho I, Yamanishi S, Cox L, Methé B a., Zavadil J, Li K, et al. Antibiotics in early life alter the murine colonic microbiome and adiposity. Nature. 2012;488(7413):621–6. [PubMed: 22914093]

32. Cox LM, Yamanishi S, Sohn J, Alekseyenko AV, Leung JM, Cho I, et al. Altering the intestinal microbiota during a critical developmental window has lasting metabolic consequences. Cell. 2014 8;158(4):705–21. [PubMed: 25126780]

33. Guss JD, Horsfield MW, Fontenele FF, Sandoval TN, Luna M, Apoorva F, et al. Alterations to the Gut Microbiome Impair Bone Strength and Tissue Material Properties. J Bone Miner Res. 2017;32(6):1343–53. [PubMed: 28244143]

34. Rodrigues FC, Castro ASB, Rodrigues VC, Fernandes SA, Fontes EAF, de Oliveira TT, et al. Yacon Flour and *Bifidobacterium longum* Modulate Bone Health in Rats. J Med Food. 2012;15(7):664–70. [PubMed: 22510044]

35. Ohlsson C, Nigro G, Boneca IG, Bäckhed F, Sansonetti P, Sjögren K. Regulation of bone mass by the gut microbiota is dependent on NOD1 and NOD2 signaling. Cell Immunol. 2017;(March):0–1.

36. Tyagi AM, Yu M, Darby TM, Vaccaro C, Li J-Y, Owens JA, et al. The Microbial Metabolite Butyrate Stimulates Bone Formation via T Regulatory Cell-Mediated Regulation of WNT10B Expression. Immunity. 2018;1–16.

37. Katono T, Kawato T, Tanabe N, Suzuki N, Iida T, Morozumi A, et al. Sodium butyrate stimulates mineralized nodule formation and osteoprotegerin expression by human osteoblasts. Arch Oral Biol. 2008;53(10):903–9. [PubMed: 18406397]

38. Dar HY, Shukla P, Mishra PK, Anupam R, Mondal RK, Tomar GB, et al. Lactobacillus acidophilus inhibits bone loss and increases bone heterogeneity in osteoporotic mice via modulating Treg-Th17 cell balance. Bone Reports. 2018;8(July 2017):46–56. [PubMed: 29955622]

39. Cani PD, Bibiloni R, Knauf C, Waget A, Neyrinck AM, Delzenne NM, et al. Changes in gut microbiota control metabolic endotoxemia-induced inflammation in high-fat diet-induced obesity and diabetes in mice. Diabetes. 2008 6;57(6):1470–81. [PubMed: 18305141]

40. Ferrier L, Bérard F, Debrauwer L, Chabo C, Langella P, Buéno L, et al. Impairment of the intestinal barrier by ethanol involves enteric microflora and mast cell activation in rodents. Am J Pathol. 2006 4;168(4):1148–54. [PubMed: 16565490]

41. Collins J, Auchtung JM, Schaefer L, Eaton KA, Britton RA. Humanized microbiota mice as a model of recurrent Clostridium difficile disease. Microbiome. 2015 Aug;3:35.

42. Kozich JJ, Westcott SL, Baxter NT, Highlander SK, Schloss PD. Development of a dual-index sequencing strategy and curation pipeline for analyzing amplicon sequence data on the MiSeq Illumina sequencing platform. Appl Environ Microbiol. 2013 9;79(17):5112–20. [PubMed: 23793624]

43. Team RC. R: a language and environment for statistical computing. R Froundation for Statistical Computing, Vienna, Austria 2017.

44. McMurdie PJ, Holmes S. phyloseq: An R Package for Reproducible Interactive Analysis and Graphics of Microbiome Census Data. Watson M, editor. PLoS One. 2013 4;8(4):e61217. [PubMed: 23630581]

45. Gardinier JD, Rostami N, Juliano L, Zhang C. Bone adaptation in response to treadmill exercise in young and adult mice. Bone reports. 2018 6;8:29–37. [PubMed: 29379848]

46. Turner CH, Burr DB. Basic biomechanical measurements of bone: A tutorial. Bone. 1993 7;14(4):595–608. [PubMed: 8274302]

47. Shi Y, Zhao X, Zhao J, Zhang H, Zhai Q, Narbad A, et al. A mixture of Lactobacillus species isolated from traditional fermented foods promote recovery from antibiotic-induced intestinal disruption in mice. J Appl Microbiol. 2018;124(3):842–54. [PubMed: 29314490]

48. Perez-Cobas AE, Gosalbes MJ, Friedrichs A, Knecht H, Artacho A, Eismann K, et al. Gut microbiota disturbance during antibiotic therapy: a multi-omic approach. Gut. 2012;62(11):1–11.

49. Langdon A, Crook N, Dantas G. The effects of antibiotics on the microbiome throughout development and alternative approaches for therapeutic modulation. Genome Med. 2016;8(1):39. [PubMed: 27074706]

Author Manuscript Author Manuscript Author Manuscript Author Manuscript

50. Kimura T, Endo H, Yoshikawa M, Muranishi S, Sezaki H. Carrier-mediated transport systems for aminopenicillins in rat small intestine. J Pharmacobiodyn. 1978;1(4):262–7.
51. Tsuji A, Nakashima E, Kagami I, Yamana T. Intestinal Absorption Mechanism of Amphoteric P-Lactam Antibiotics I: Comparative Absorption and Evidence for In Situ Rat Small Intestine. 1981;70(7).
52. Van Der Waaij D, Berghuis-de Vries JM, Korthals Altes C. Oral dose and faecal concentration of antibiotics during antibiotic decontamination in mice and in a patient. J Hyg (Lond). 1974;73(2):197–203. [PubMed: 4528886]
53. Kim J-I, Park J-S, Kim H, Ryu S-K, Kwak J, Kwon E, et al. CRISPR/Cas9-mediated knockout of Rag-2 causes systemic lymphopenia with hypoplastic lymphoid organs in FVB mice. Lab Anim Res. 2018;34(4):166. [PubMed: 30671102]
54. Mann ER, Andersen P, Alcon-giner C, Leclaire C, Caim S, Wessel H, et al. Antibiotics induce sustained dysregulation of intestinal T-cell immunity by perturbing macrophage homeostasis. :1–16.
55. Zarrinpar A, Chaix A, Xu ZZ, Chang MW, Marotz CA, Saghatelian A, et al. Antibiotic-induced microbiome depletion alters metabolic homeostasis by affecting gut signaling and colonic metabolism. Nat Commun. 2018;9(1):2872. [PubMed: 30030441]
56. Ge X, Ding C, Zhao W, Xu L, Tian H, Gong J, et al. Antibiotics-induced depletion of mice microbiota induces changes in host serotonin biosynthesis and intestinal motility. J Transl Med. 2017;15(1):1–9. [PubMed: 28049494]
57. Ubeda C, Pamer EG. Antibiotics, microbiota, and immune defense. Trends Immunol. 2012 9;33(9):459–66. [PubMed: 22677185]
58. Jin Y, Wu Y, Zeng Z, Jin C, Wu S, Wang Y, et al. Exposure to Oral Antibiotics Induces Gut Microbiota Dysbiosis Associated with Lipid Metabolism Dysfunction and Low-Grade Inflammation in Mice.
59. Francino MP, Moya A. Effects of Antibiotic Use on the Microbiota of the Gut and Associated Alterations of Immunity and Metabolism. EMJ Gastroenterol. 2013;1(December):74–80.
60. Klausen B, Hougen HP, Fiehn N-E. Increased periodontal bone loss in temporarily B lymphocyte-deficient rats. J Periodontal Res. 1989;24(6):384–90. [PubMed: 2531793]
61. Li Y, Toraldo G, Li A, Yang X, Zhang H, Qian WP, et al. B cells and T cells are critical for the preservation of bone homeostasis and attainment of peak bone mass in vivo. Blood. 2007;109(9):3839–48. [PubMed: 17202317]
62. Sun W, Meednu N, Rosenberg A, Rangel-Moreno J, Wang V, Glanzman J, et al. B cells inhibit bone formation in rheumatoid arthritis by suppressing osteoblast differentiation. Nat Commun. 2018;9(1):5127. [PubMed: 30510188]
63. Zhang YH, Heulsmann A, Tondravi MM, Mukherjee A, Abu-Amer Y. Tumor necrosis factor-α (TNF) stimulates RANKL-induced osteoclastogenesis via coupling of TNF type 1 receptor and RANK signaling pathways. J Biol Chem. 2001 1;276(1):563–8. [PubMed: 11032840]
64. Wang LM, Zhao N, Zhang J, Sun QF, Yang CZ, Yang PS. Tumor necrosis factor-alpha inhibits osteogenic differentiation of pre-osteoblasts by downregulation of EphB4 signaling via activated nuclear factor-kappaB signaling pathway. J Periodontal Res. 2018;53(1):66–72. [PubMed: 28857167]
65. Kim JW, Lee MS, Lee CH, Kim HY, Chae SU, Kwak HB, et al. Effect of interferon- γ on the fusion of mononuclear osteoclasts into bone-resorbing osteoclasts. BMB Rep. 2012;
66. Gao Y, Grassi F, Ryan MR, Terauchi M, Page K, Yang X, et al. IFN-gamma stimulates osteoclast formation and bone loss in vivo via antigen-driven T cell activation. J Clin Invest. 2007;117(1):122–32. [PubMed: 17173138]
67. Adamopoulos IE, Chao C chi, Geissler R, Laface D, Blumenschein W, Iwakura Y, et al. Interleukin-17A upregulates receptor activator of NF-κB on osteoclast precursors. Arthritis Res Ther. 2010;12(1):1–11.
68. Xu LX, Kukita T, Kukita A, Otsuka T, Niho Y, Iijima T. Interleukin- 10 selectively inhibits osteoclastogenesis by inhibiting differentiation of osteoclast progenitors into preosteoclast- like cells in rat bone marrow culture system. J Cell Physiol. 1995 12;165(3):624–9. [PubMed: 7593242]

Author Manuscript Author Manuscript Author Manuscript Author Manuscript

69. Mohamed SGK, Sugiyama E, Shinoda K, Taki H, Hounoki H, Abdel-Aziz HO, et al. Interleukin-10 inhibits RANKL-mediated expression of NFATc1 in part via suppression of c-Fos and c-Jun in RAW264.7 cells and mouse bone marrow cells. Bone. 2007;41(4):592–602. [PubMed: 17627913]

70. Zaiss MM, Axmann R, Zwerina J, Polzer K, Gückel E, Skapenko A, et al. Treg cells suppress osteoclast formation: A new link between the immune system and bone. Arthritis Rheum. 2007;56(12):4104–12. [PubMed: 18050211]

71. Collins FL, Rios-Arce ND, Schepper JD, Jones AD, Schaefer L, Britton RA, et al. Beneficial effects of Lactobacillus reuteri 6475 on bone density in male mice is dependent on lymphocytes. Sci Rep. 2019;

72. Jakobsson HE, Jernberg C, Andersson AAF, Sjölund-Karlsson M, Jansson JJK, Engstrand L, et al. Short-Term Antibiotic Treatment Has Differing Long-Term Impacts on the Human Throat and Gut Microbiome. Ratner AJ, editor. PLoS One. 2010 3;5(3):e9836. [PubMed: 20352091]

73. Jernberg C, Löfmark S, Edlund C, Jansson JK. Long-term ecological impacts of antibiotic administration on the human intestinal microbiota. ISME J. 2007 5;1(1):56–66. [PubMed: 18043614]

74. Miyoshi J, Bobe AM, Miyoshi S, Huang Y, Hubert N, Delmont TO, et al. Peripartum Antibiotics Promote Gut Dysbiosis, Loss of Immune Tolerance, and Inflammatory Bowel Disease in Genetically Prone Offspring. Cell Rep. 2017 7;20(2):491–504. [PubMed: 28700948]

75. Becattini S, Taur Y, Pamer EG. Antibiotic-Induced Changes in the Intestinal Microbiota and Disease. Vol. 22, Trends in Molecular Medicine. 2016 p. 458–78. [PubMed: 27178527]

76. Gálvez EJC, Iljazovic A, Gronow A, Flavell R, Strowig T. Shaping of Intestinal Microbiota in Nlrp6- and Rag2-Deficient Mice Depends on Community Structure. Cell Rep. 2017;21(13):3914–26. [PubMed: 29281837]

77. Zhang H, Sparks JB, Karyala SV., Settlage R, Luo XM. Host adaptive immunity alters gut microbiota. ISME J. 2015;9(3):770–81. [PubMed: 25216087]

78. Chiang S-S, Pan T-M. Antiosteoporotic effects of Lactobacillus -fermented soy skim milk on bone mineral density and the microstructure of femoral bone in ovariectomized mice. J Agric Food Chem. 2011;59(14):7734–42. [PubMed: 21668014]

79. Kim JG, Lee E, Kim SH, Whang KY, Oh S, Imm JY. Effects of a Lactobacillus casei 393 fermented milk product on bone metabolism in ovariectomised rats. Int Dairy J. 2009;19(11):690–5.

80. Schepper JD et al. Involvement of the gut microbiota and barrier function in glucocorticoid induced osteoporosis. J Bone Miner Res. 2019;

81. Li J-Y, Chassaing B, Tyagi AM, Vaccaro C, Luo T, Adams J, et al. Sex steroid deficiency–associated bone loss is microbiota dependent and prevented by probiotics. J Clin Invest. 2016 4;126(6):2049–63. [PubMed: 27111232]

82. Winter S, Ratner A, Nelson A, Weiser J, Benoist C, Mathis D. Deciphering the tête-à-tête between the microbiota and the immune system. Nature. 2014 10;467(7314):426–9.

Author Manuscript Author Manuscript Author Manuscript Author Manuscript

Highlights:

- Antibiotic-induced dysbiosis causes bone loss in multiple strains of mice.
- Dysbiosis-induced bone loss is dependent on T and B lymphocytes in mice.
- Bacterial repopulation following antibiotic treatment is different between wild type and lymphocyte deficient mice.
- *L. reuteri* supplementation prevents dysbiosis-induced bone loss in mice.

Author Manuscript Author Manuscript Author Manuscript Author Manuscript

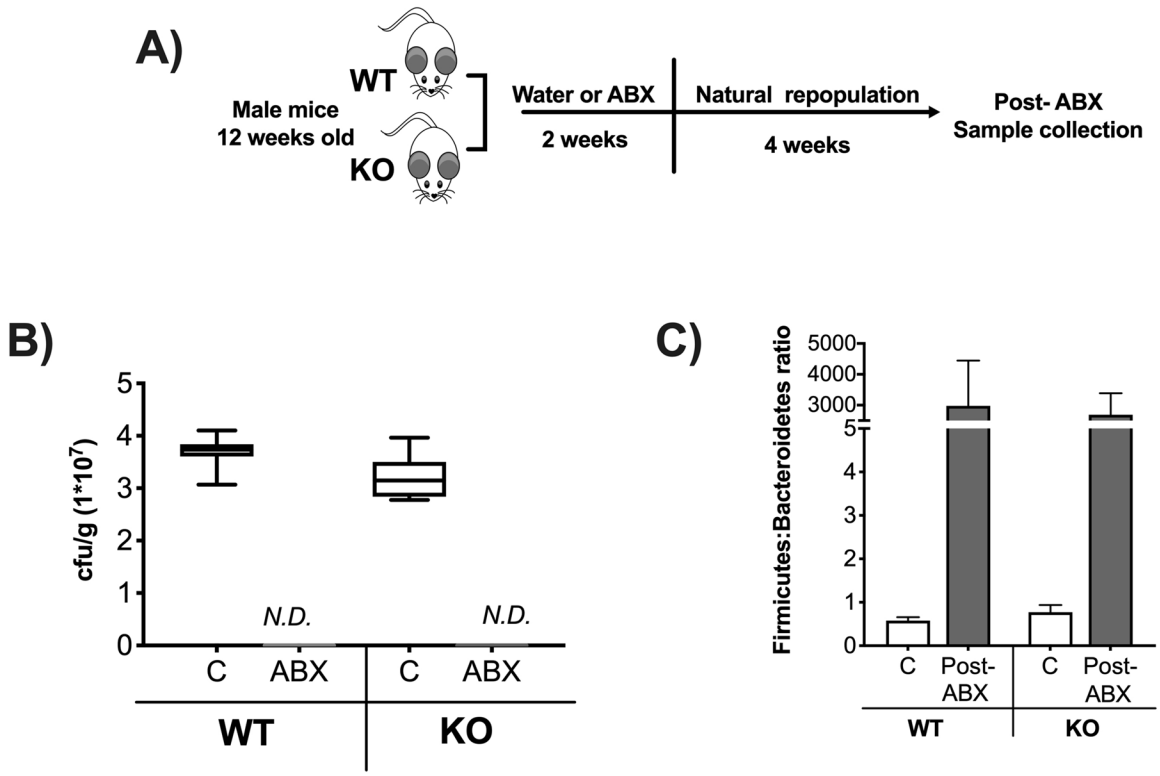

Figure 1. Two weeks antibiotic treatment decreases fecal microbiota composition.

12-week-old C57BL/6 and Rag2-KO male mice were treated with water or the antibiotics (ABX) ampicillin and neomycin in the drinking water for 2-weeks followed by 4 weeks of no treatment (repopulation). **A)** Experimental design. **B)** Fecal samples were plated in agar dishes for 24 hours under anaerobic conditions to determine number of colony forming units per gram of feces (cfu/g). Control samples were diluted 1:7 while ABX were undiluted. **C)** Relative abundance of Firmicutes to Bacteroidetes ratio in colonic fecal samples after 4 weeks of no treatment (repopulation). Whiskers in the box plot represent 5–95 percentile. n=9–14 per group. C: control, ABX: antibiotic treated for 2 weeks, Post-ABX: antibiotic treated for 2 weeks followed by 4 weeks of no treatment. WT: wild type, KO: Rag2 KO.

Author Manuscript Author Manuscript Author Manuscript Author Manuscript

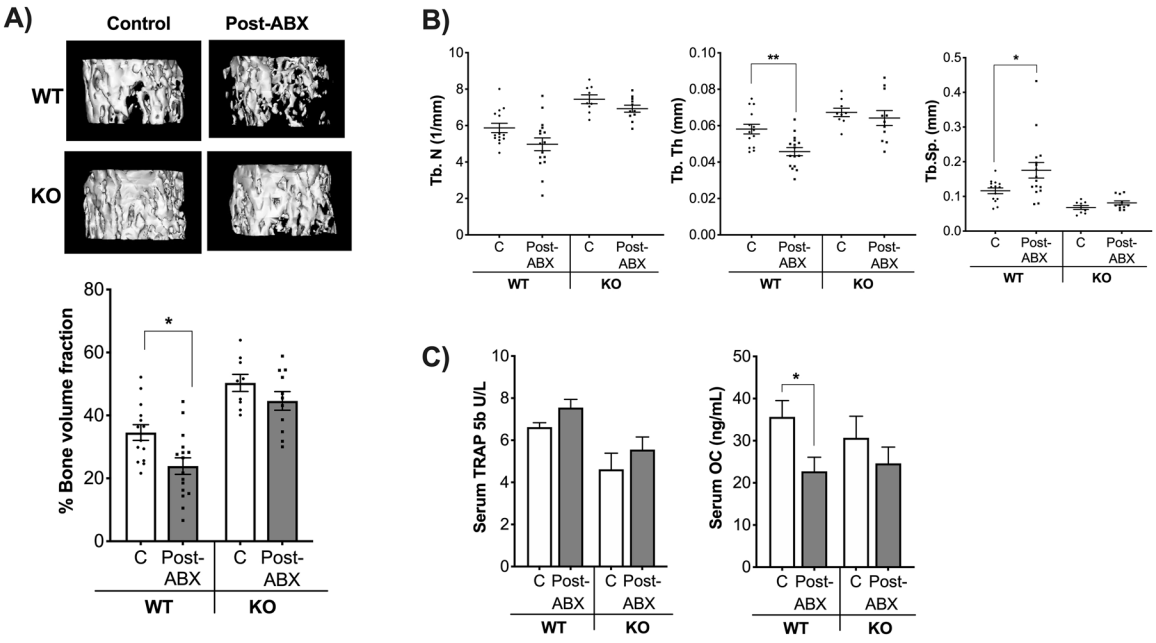

Figure 2. Gut microbiota repopulation effects on femoral trabecular bone density require the T and B lymphocytes.

12-week-old C57BL/6 and Rag2-KO male mice were treated with water or antibiotics (ABX) for 2-weeks followed by 4 weeks of no treatment (repopulation). Colonic fecal samples were collected from these mice and analyzed by 16S RNA assay. **A)** Representative micro-computed tomography isosurface images by uCT and percentage of femoral bone volume fraction (%BVF); n=9–17 per group. **B)** Trabecular number (Tb. N (1/mm)), trabecular thickness (Tb. Th (mm)), and trabecular space (Tb. Sp (mm)). **C)** Serum tartrate-resistance acid phosphatase levels (TRAP 5b(U/L)) and serum osteocalcin levels (OC (mg/mL)); n=5–17 per group. Values represent mean ± standard error. Statistical analysis performed by 1-way ANOVA with Tukey post-test. ****p<0.0001, **p<0.01, *p<0.05. Note that for Fig 2C serum TRAP5b levels, C and Post-ABX groups in the WT mice were significantly different based on unpaired t-test (p=0.03). C: control, Post-ABX: antibiotic treated for 2 weeks followed by 4 weeks of no treatment. WT: wild type, KO: Rag2 KO. Outliers removed by the ROUT test (Q:0.1%): Serum OC; one in the KO-C and one in the KO-Post ABX. Serum TRAP; one in the WT-C. None of the outliers removed affected the significance of the results.

Author Manuscript Author Manuscript Author Manuscript Author Manuscript

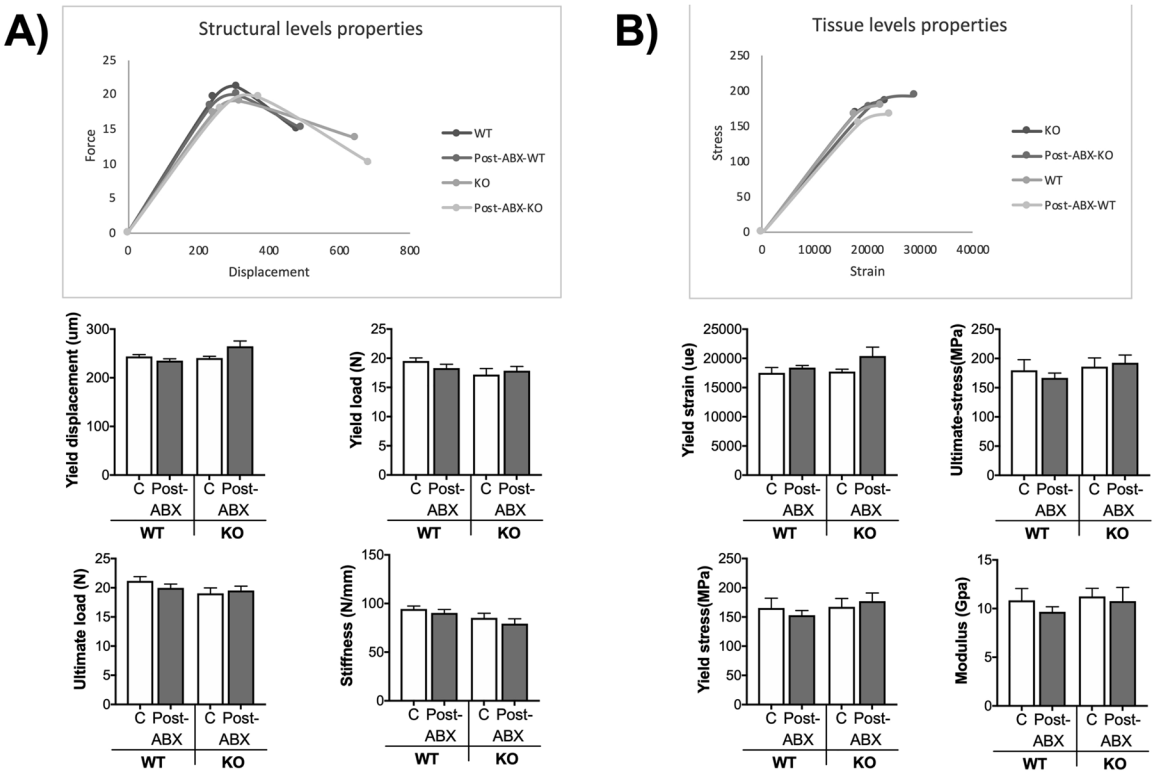

Figure 3. Microbial manipulation does not alter mechanical bone properties.

Analysis of tibia mechanical properties from mice described in figure 2 were performed by four-point bending test. **A)** Structural levels properties. **B)** Tissue level properties. Values represent mean ± standard error. n= 12–18 per group. C: control, Post-ABX: antibiotic treated for 2 weeks followed by 4 weeks of no treatment. WT: wild type, KO: Rag2 KO.

Author Manuscript Author Manuscript Author Manuscript Author Manuscript

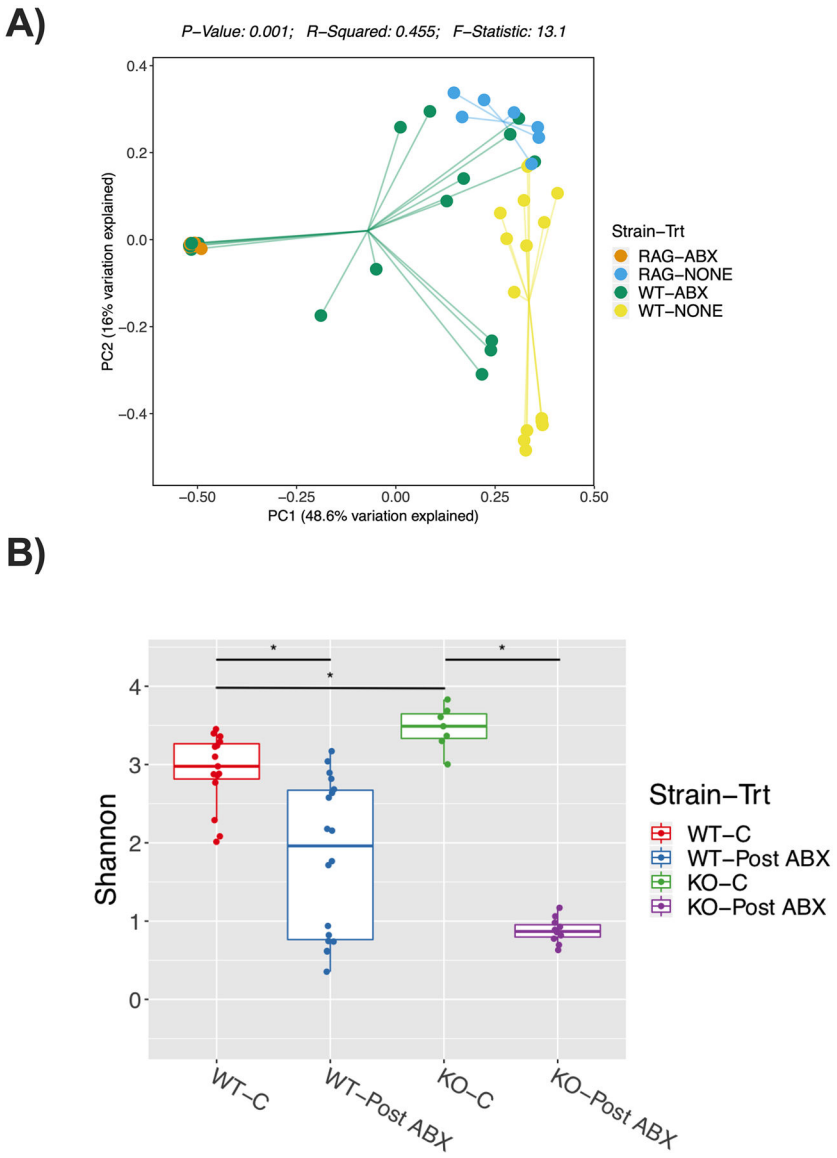

Figure 4. Microbiota analysis of colonic fecal samples following post-antibiotic treatment

12-week-old C57BL/6 and Rag2-KO male mice were treated with water or antibiotics (ABX) for 2-weeks followed by 4 weeks of no treatment (repopulation). Colonic fecal samples were collected from these mice and analyzed by 16S sequencing. Principal co-ordinates analysis (PCoA) plot of fecal microbiome, **A)** Bray-Curtis analysis performed; The F-statistic provides information on the degree of effect caused by the antibiotic treatment, the p-value reflects the certainty of the F-statistic given the data, and R^2 reflects the overall ability of the model to explain all of the data. **B)** Shannon Diversity. Statistical analysis was done using Mann-Whitney U test and P-values were adjusted using Benjamini and Hochberg's method with FDR of <0.05. * refers to p<0.005. Values represent mean ± standard error. n=7–17 per group. C: control, Post-ABX: antibiotic treated for 2 weeks followed by 4 weeks of no treatment. WT: wild type, KO: Rag2 KO.

Author Manuscript Author Manuscript Author Manuscript Author Manuscript

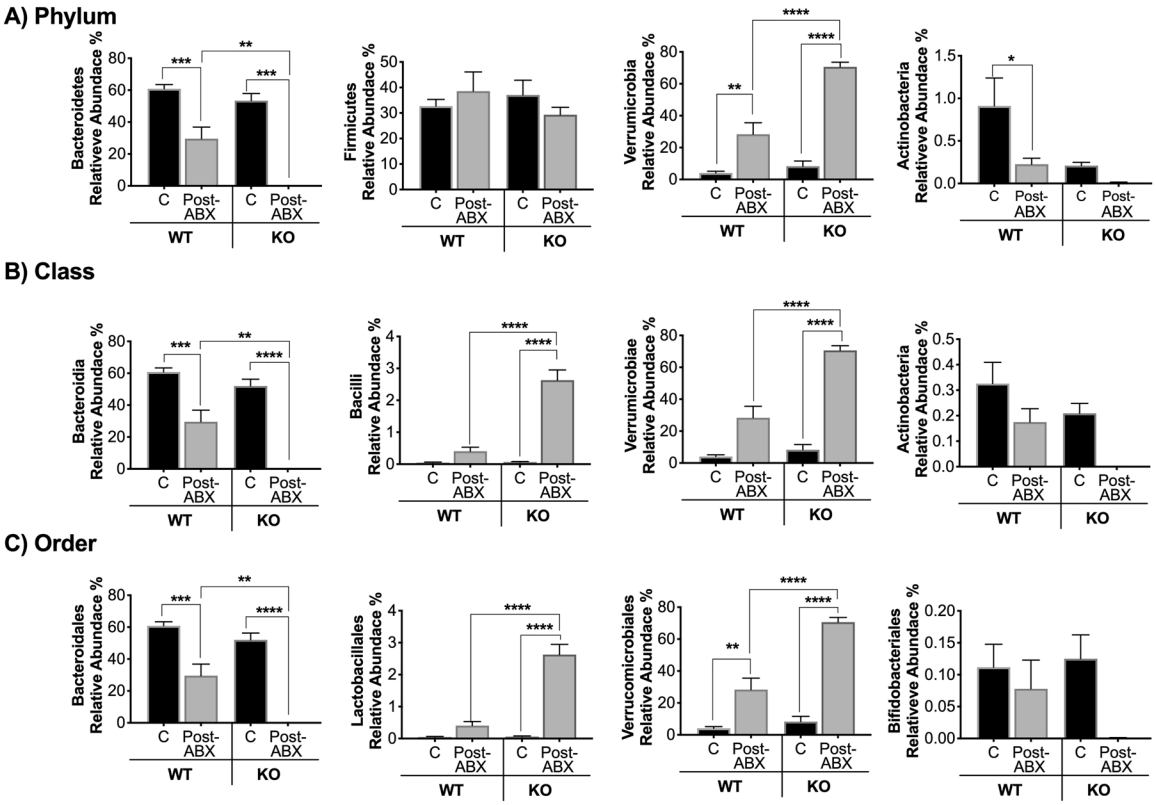

Figure 5. Relative abundance of specific bacteria post-antibiotic treatment.

Colon fecal samples from C57BL/6 and Rag2-KO treated mice (ABX for 2 weeks and repopulation for 4 weeks) were collected and analyzed. **A)** Analysis of operational taxonomic units (OTUs) classified to the phylum **B)** class, and **C)** order level. Values represent mean ± standard error. n > 7 per group. Statistical analysis performed by 1-way ANOVA with Tukey post-test. ****p<0.0001, **p<0.01, *p<0.05. C: control, Post-ABX: antibiotic treated for 2 weeks followed by 4 weeks of no treatment. WT: wild type, KO: Rag-KO. Outliers removed by the ROUT test (Q:0.1%): Class Actinobacteria; three in the WT:C, one in the WT-Post-Abx and one in the KO-Post-ABX. Order Lactobacillales; one in the WT-C and three in the WT-Post-Abx. Family Lactobacillaceae; one in the WT-C, three in the WT-Post-Abx and one in the KO-Post-ABX.

Author Manuscript Author Manuscript Author Manuscript Author Manuscript

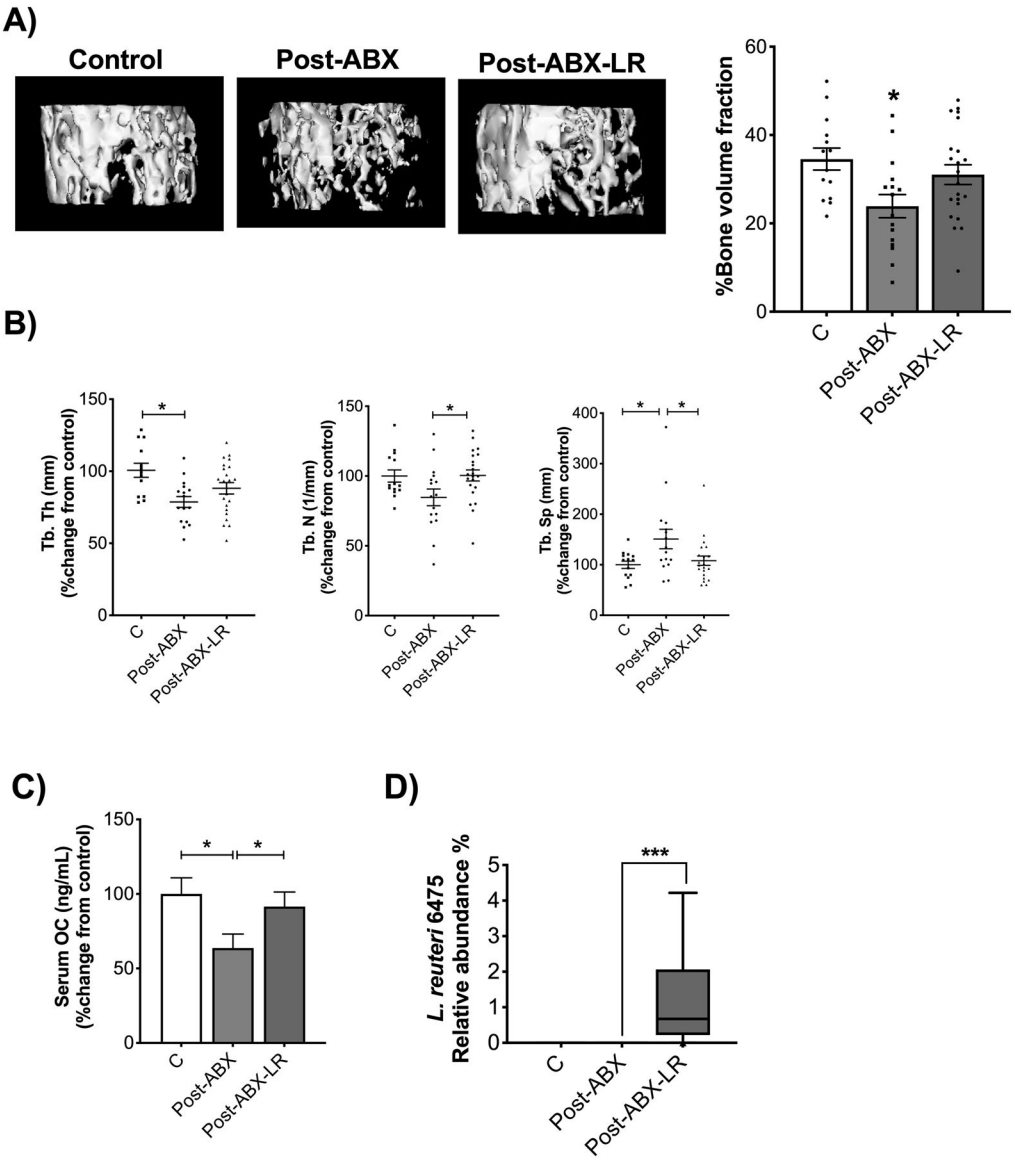

Figure 6. Supplementation with *Lactobacillus reuteri* 6475 prevents bone loss in post-antibiotic treated C57BL/6 male mice.

After treatment with ABX for two weeks WT male mice were untreated (natural repopulation, group shown in Fig 2) or treated with *L. reuteri* 6475 for four weeks. Note that the C and Post-ABX are the same as shown in Fig 2. These experiments were done together with the LR supplementation group. **A)** Representative micro-computed tomography isosurface images by uCT. **B)** Trabecular thickness (Tb. Th (mm)), trabecular number (Tb. N (1/mm)), and trabecular space (Tb. Sp (mm)) expressed as percentage change from control. **C)** Serum osteocalcin levels (OC (mg/mL)) expressed as percentage change from control. **D)** Analysis of relative abundance of *L. reuteri* 6475. Values represent mean ± standard error. n > 7 per group. Statistical analysis performed by T-test or 1-way ANOVA with Tukey post-test. *p<0.05 compared to control. Control and Post-ABX-LR are not significantly different.

C: control, Post-ABX: antibiotic treated for 2 weeks followed by 4 weeks of no treatment, Post-ABX-LR: antibiotic treated for 2 weeks followed by 4 weeks of LR.

Author Manuscript Author Manuscript Author Manuscript Author Manuscript

Author Manuscript

Author Manuscript

Author Manuscript

Author Manuscript

Table 1:

General mouse parameters post-ABX treatment

General mouse parameters				
	WT		KO	
Parameters	C	Post-ABX	C	Post-ABX
	(n=14)	(n=17)	(n=9)	(n=11)
Body weight (g)	35.09 ± 1.07	34.31 ± 1.32	32.06 ± 0.88	30.15 ± 0.70
Cecum (g)	0.69 ± 0.03	1.03 ± 0.15	0.64 ± 0.03	1.53 ± 0.16 #
Liver (g)	1.63 ± 0.04	1.75 ± 0.08	1.60 ± 0.03	1.50 ± 0.05
Kidney (g)	0.22 ± 0.09	0.21 ± 0.01	0.22 ± 0.01	0.21 ± 0.02
Spleen (g)	0.091 ± 0.003	0.087 ± 0.004	0.034 ± 0.002 *	0.049 ± 0.004 *

Author Manuscript Author Manuscript Author Manuscript Author Manuscript

Table 2:

Bone parameter post-ABX treatment

Femoral Bone Parameters					
	WT			KO	
Parameter	C (n=14)	Post-ABX (n=17)	Post-ABX LR (n=22)	C (n=9)	Post-ABX (n=11)
Femur trabecular					
BV/TV	34.42 ± 2.49	25.25 ± 2.85 *	30.91 ± 2.22 (^0.09)	50.21 ± 2.72 *	44.47 ± 2.97
BMD (mg/mL)	286.7 ± 11.07	243.1 ± 13.15 *	277.5 ± 11.02	311.1 ± 15.59	326.4 ± 15.26
BMC (mg)	0.9532 ± 0.045	0.7936 ± 0.043	0.8895 ± 0.045	1.00 ± 0.077	1.046 ± 0.056
Tb. Th. (mm)	0.058 ± 0.002	0.047 ± 0.002 *	0.051 ± 0.002	0.067 ± 0.002	0.064 ± 0.004
Tb. N.(1/mm)	5.87 ± 0.25	5.06 ± 0.34	5.89 ± 0.23 ^	7.44 ± 0.24 *	6.92 ± 0.19
Tb. Sp. (mm)	0.112 ± 0.008	0.1698 ± 0.005 *	0.117 ± 0.007 ^	0.068 ± 0.005	0.081 ± 0.005
Femur Cortical					
Ct.Ar (mm^2)	1.01 ± 0.01	0.94 ± 0.02	0.97 ± 0.02	0.96 ± 0.05	1.00 ± 0.03
Ct.Th (mm)	0.23 ± 0.005	0.22 ± 0.004	0.22 ± 0.004	0.23 ± 0.006	0.23 ± 0.009
Ma.Ar (mm^2)	1.07 ± 0.04	1.08 ± 0.03	1.05 ± 0.03	1.03 ± 0.05	1.02 ± 0.04
Tt.Ar (mm^2)	2.09 ± 0.04	2.03 ± 0.03	2.02 ± 0.04	2.00 ± 0.09	2.02 ± 0.07
Inner perimeter (mm)	3.93 ± 0.080	3.99 ± 0.06	3.91 ± 0.06	3.83 ± 0.12	3.80 ± 0.09
Outer perimeter (mm)	5.39 ± 0.05	5.42 ± 0.11	5.30 ± 0.05	5.25 ± 0.14	5.34 ± 0.14
BMD (mg/cc)	964.8 ± 18.37	931.2 ± 18.57	930 ± 11.17	928.6 ± 21.47	965.4 ± 25.24
BMC (mg)	0.019 ± 0.0004	0.017 ± 0.0005	0.018 ± 0.0005	0.018 ± 0.001	0.019 ± 0.001